JOURNAL OF MAGNETIC RESONANCE **131,** 25–31 (1998)
ARTICLE NO. MN971320

Multiecho Imaging with Suboptimal Spoiler Gradients[1]

Mark D. Does[2] and Richard E. Snyder

Department of Biomedical Engineering, University of Alberta, Edmonton, Alberta, Canada T6G 2G3

Received June 13, 1997; revised October 24, 1997

Although multiecho imaging may be used to measure transverse relaxation (T_2), B_1 and B_0 inhomogeneity generally gives rise to unwanted coherence pathway signals which result in erroneous T_2 measurements. One approach to suppressing this unwanted signal is to center each rf refocusing pulse between spoiler gradients which dephase the unwanted signal; however, hardware limitations often dictate the use of suboptimal spoiler gradients, that is, gradients that cannot provide sufficient dephasing strength. Using simulations, this work demonstrates that by means of a small additional spoiler gradient prior to the first rf refocusing pulse it is possible to reduce substantially the contribution from unwanted coherence pathways in multiecho imaging studies that use suboptimal spoiler gradients. This reduction of unwanted signal results in measured T_2 values within ≈1% of values obtained using spoiler gradients of optimal strength. These results were found for a wide range of biologically relevant T_1 and T_2 values, missettings of the rf refocusing pulse as large as 5%, and frequency offsets of up to 25 Hz. Multiecho image data agreed with the simulations. Using the additional spoiler gradient it is possible to reduce spoiler gradient strengths by up to 75%. © 1998 Academic Press

Key Words: **magnetic resonance imaging; transverse (T_2) relaxation; multiecho imaging; spoiler gradients.**

INTRODUCTION

It is often desirable to be able to measure transverse relaxation (T_2) *in vivo* using a multiecho magnetic resonance imaging protocol; however, implementing such a measurement is fraught with difficulty. Imperfections in multiecho imaging arise due to B_1 and B_0 inhomogeneity which results in imperfect refocusing of magnetization. Over the course of several echoes the fraction of magnetization that does not experience the desired evolution becomes sizable and, consequently, interferes with the desired signal. The objective, then, of approaches to measuring T_2 accurately using a multiecho imaging sequence is to eliminate this unwanted fraction of the signal.

One such approach is to dephase the unwanted signal using a pair of spoiler gradients centered around each rf refocusing pulse. The area of each gradient pulse must be adjusted so that unwanted magnetization dephased by one spoiler will not be rephased by a later spoiler. Such a pattern of spoiler gradients has been developed (*1*), but despite this pattern being optimized to require minimal gradient strengths most gradient hardware systems are unable to achieve the gradient strengths required in many multiecho imaging situations, resulting in incomplete dephasing of unwanted signal. Although a modification to this spoiler pattern has been proposed for the case of suboptimal spoiler gradient strengths (*2*), no quantitative investigation into the implications of using suboptimal spoiler strengths has been published. This work demonstrates that when hardware limitations dictate the use of suboptimal spoiler gradients, a small adjustment to the strength of the first spoiler gradient can greatly compensate for the deleterious effects of the insufficient spoiler gradients.

SPOILER GRADIENTS

The objective of a given pattern of spoiler gradients is to suppress signal arising from selected coherence pathways. For the simple case of a rectangular, homogenous slice, the reduction of observable magnetization due to a single slice-direction spoiler gradient pulse is a sinc function of half the gradient dephasing strength (*3*); therefore, it is ideal for all unwanted coherence pathways to experience a net dephasing of $\pm 2m\pi$ radians across the slice ($m = 1, 2, \ldots$) and the desired coherence pathway(s) to experience zero net dephasing. In the case of multiecho imaging it is desirable to preserve only the spin-echo pathway. In general, this can be achieved by placing a pair of identical spoiler gradients around each refocusing pulse. The strength of each pair must be adjusted so that no stimulated echo dephased by one spoiler gradient will be rephased by a later spoiler gradient. The pattern of spoiler gradient pairs proposed in Ref. (*2*), as shown in Fig. 1 for the case of $S_{\text{add}} = 0$, completely dephases magnetization arising from all unwanted pathways in a multiecho imaging sequence of NE echoes as long as the smallest spoiler strength, S_{min}, equals $\pm 2m\pi$. However,

[1] This work was presented in part at the 5th Annual Meeting of the International Society of Magnetic Resonance in Medicine, April 1997, Vancouver.

[2] Now at Department of Diagnostic Radiology, Yale University, New Haven, CT 06511.

1090-7807/98 $25.00

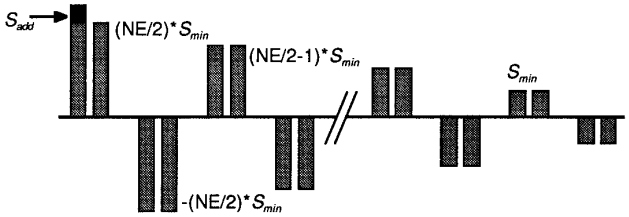

FIG. 1. Spoiler gradient pattern for quantitative multiecho imaging. The grey bars depict the spoiler gradients proposed in Ref. 2, and the black bar is the addition to the first spoiler defined in the text as S_{add}.

this spoiler gradient sequence requires a maximum spoiler dephasing strength of $(NE/2) \times S_{min}$. When a large NE, short echo time (TE), and/or thin imaging slice is required, many gradient hardware systems are unable to achieve this maximum spoiler strength, resulting in erroneous T_2 measurements. For example, in multiecho imaging with an echo time of 20 ms, it is unlikely to be possible to use spoiler pulses longer than $\approx$4 ms in duration. Assuming a slice thickness of 5 mm and a maximum gradient amplitude of 1 G/cm, the maximum spoiler could dephase no more than $\approx 17\pi$ across the slice. Therefore, for NE > 16 it would not be possible to completely eliminate signal from all unwanted coherence pathways.

The fact that all unwanted pathways cannot be completely eliminated, however, does not mean that the net signal from the unwanted pathways cannot be reduced to a tolerable level. For reasonably small rf pulse imperfections the vast majority of the unwanted pathways do not contribute a significant amount to the observed echo, and some of those that do will add destructively with others. In the following, it is shown using computer simulated data and experimentally acquired data that increasing the spoiler gradient prior to the first rf refocussing pulse by an additional strength S_{add} ($<2\pi$) (Fig. 1) can increase the amount of mutual cancellation amongst the unwanted coherence pathways when $S_{min} < 2\pi$, thereby reducing the contamination of spin-echo data at the expense of a somewhat reduced signal-to-noise ratio. This small adjustment to the spoiler gradient pattern greatly reduces the maximum spoiler strength required to achieve acceptable T_2 measurements.

METHODS AND RESULTS

Coherence Pathway Simulations

For a given echo in a multiecho imaging sequence, the observed signal can be decomposed into contributions from different coherence pathways. Using the method described by Simbrunner (*4*), a generalization of earlier methods (*5–7*), the observable magnetization at time $t = n \times$ TE ($n = 1, 2, \ldots$) can be computed for each coherence pathway. For the eighth echo there are 750 such pathways that may contribute, and these pathways can be grouped into three categories: true-T_2, T_1-artefact, and phase-artefact (assuming the case of spin-warp imaging) (*1*). The contributions from the true-T_2 and the T_1-artefact pathways add together to generate the primary image, while the signal from the phase-artefact pathway generates a ghost image. If there are phase artefacts, without a prior knowledge of the sample both at a given point in space, (x_0, y_0), and at the ghost image location, $(x_0, -y_0)$, the observed signal from that point in space cannot be predicted. For the case of the computer simulations presented, the observed signal (M_{OBS}) is defined as the sum of the signals from the true-T_2 (M_{T2}) and T_1-artefact (M_{T1}) pathways. The phase artefact signal (M_P) is tabulated independently as an estimate of the potential ghost image contribution to the true observed signal at a given point in space.

Coherence pathway simulations were performed using the parameters given in Table 1. A rectangular, homogeneous slice and a CPMG rf phase pattern were used for all simulations. For each value of S_{min} tested (Figs. 2–4) simulations were computed using 201 values of S_{add} equally spaced between 0 and 2π. From each set of M_{OBS} values that were generated, a T_{2OBS} was calculated using a least-squares fit to a single exponential. Figure 2 shows T_{2OBS} as a function of S_{add} for four values of S_{min}. The horizontal line is T_{2OBS} for the case of ideal spoiler gradients, $S_{min} = \pm 2m\pi$, a value that will henceforth be referred to as the optimal T_{2OBS}, or simply T_{2OPT}. The remaining four curves represent cases of suboptimal spoiler gradients. (Note that T_{2OPT} will always be less than T_2 because of irreversible losses imparted by imperfect refocusing pulses.) From the same collection of simulations is plotted the mean fractional contribution per

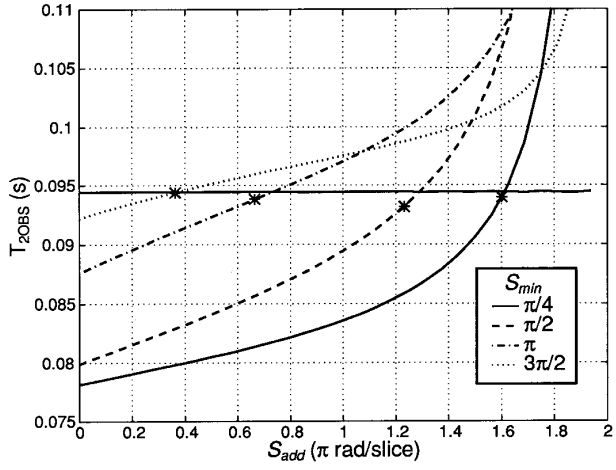

FIG. 2. Observed T_2s as a function of the spoiler adjustment, S_{add}, for four cases of minimum spoiler gradient strength, using the rf missetting listed in Table 1, and assuming a T_2 of 0.100 s. Horizontal solid line is T_{2OBS} for the case of ideal spoiler gradients; $S_{min} = \pm 2m\pi$ ($m = 0, 1, 2, \ldots$). Asterisks represent S_{add} values that result in minimal T_1-artefact corruption for corresponding S_{min} as seen in Fig. 3.

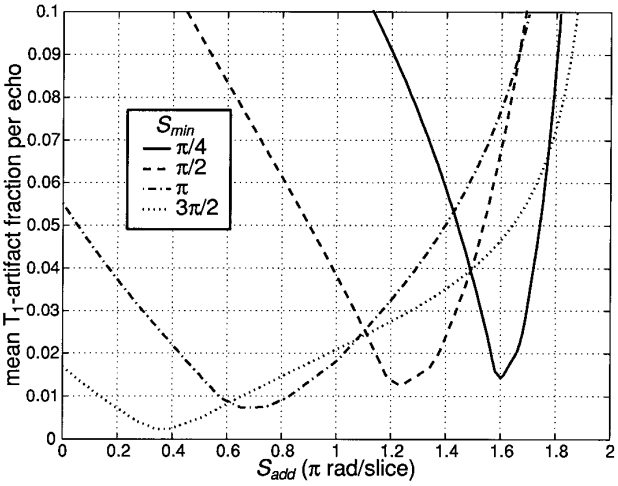

FIG. 3. Mean contribution per echo of magnetization from the T_1-artefact pathways as a function of the spoiler adjustment, S_{add}, for four cases of minimum spoiler gradient strength.

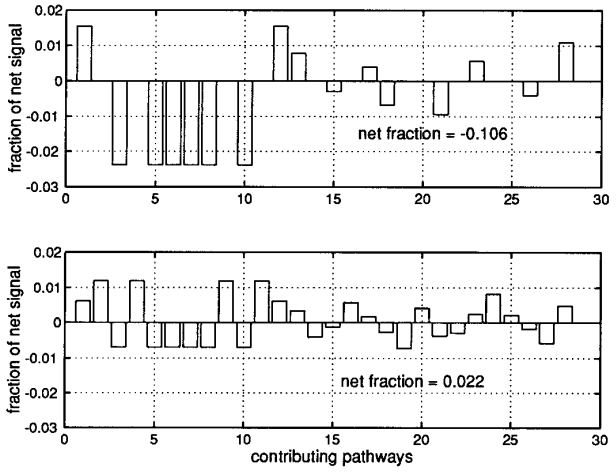

FIG. 5. Amplitudes of unwanted pathways contributing to the eighth echo under the condition $S_{\text{min}} = \pi$ and (top) $S_{\text{add}} = 0$, (bottom) $S_{\text{add}} = 0.7\pi$. Only unwanted pathways with amplitudes >0.1% of the echo amplitude are shown. Twenty-eight such pathways were found for the case of $S_{\text{add}} = 0.7\pi$ and are arranged along the abscissa (bottom), while only 16 of these same pathways were found for the case of $S_{\text{add}} = 0$ (top). The ordinate gives the amplitude of each pathway echo as a fraction of the total observed echo magnitude. A negative fraction occurs when the echo is 180° out of phase with the true-T_2 echo.

echo (i.e., the average over all eight echoes) of the M_{T1} pathways to M_{OBS} as a function of S_{add} (Fig. 3). In Fig. 4 the corresponding amount of M_{P} is shown for each of the four cases of suboptimal spoilers. The asterisk on each of these curves identifies the S_{add} adjustment required to minimize M_{T1} (Fig. 3) for that case of S_{min}.

Figure 5a shows the amplitudes of all unwanted coherence pathways with magnitudes >0.1% of the observed magnitude of the eighth echo for the case of $S_{\text{min}} = \pi$ and $S_{\text{add}} = 0$. Figure 5b shows the corresponding data that results when the first spoiler gradient is increased by $S_{\text{add}} = 0.7\pi$, i.e., the value of S_{add} required to minimize M_{T1} for the case of $S_{\text{min}} = \pi$. In each plot the net magnitude of the unwanted pathways is stated as a fraction of the observed echo magnitude.

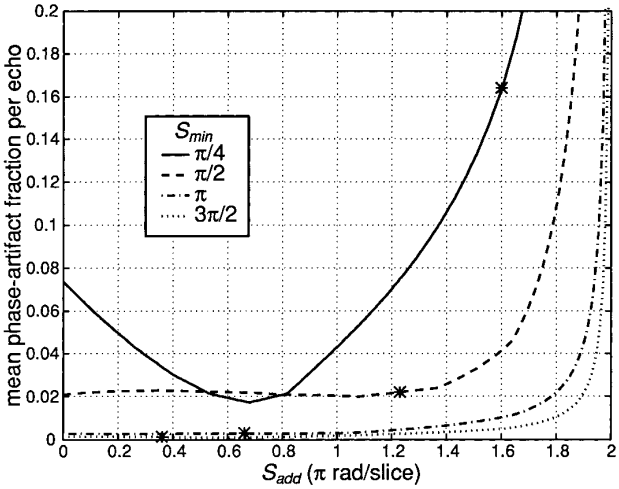

FIG. 4. Mean contribution per echo of magnetization from the phase-artefact pathways as a function of the spoiler adjustment, S_{add}, for four cases of minimum spoiler gradient. Asterisks represent S_{add} values that result in minimal T_1-artefact corruption for corresponding S_{min} as seen in Fig. 3.

Bulk-Magnetization Simulations

In order to investigate the effects of S_{add} under the condition of large NE, bulk-magnetization simulations (i.e., using the Bloch equations) were employed because it is computationally impractical to perform full coherence pathway simulations for a multiecho sequence when NE becomes large. The results of multiecho simulations using parameters given in Table 1 for three spoiler gradient settings are shown in

TABLE 1
Multiecho Imaging Parameters Used in Computer Simulations

Parameter[a]	Coherence pathway	Bulk magnetization
NE	8	32
TE (ms)	20	20
R_1 (s^{-1})	1.0	0.5
R_2 (s^{-1})	10	5
B_1 amplitude (Hz)	333	333
B_{OFF} (Hz)	25	25
B_{MIS} (%)	5	5

Note. NE = number of echoes, TE = echo time, R_1 = longitudinal relaxation rate, R_2 = transverse relaxation rate, B_{OFF} = offset frequency from resonance of rf refocusing pulse, B_{MIS} = amplitude missetting of rf refocusing pulse.

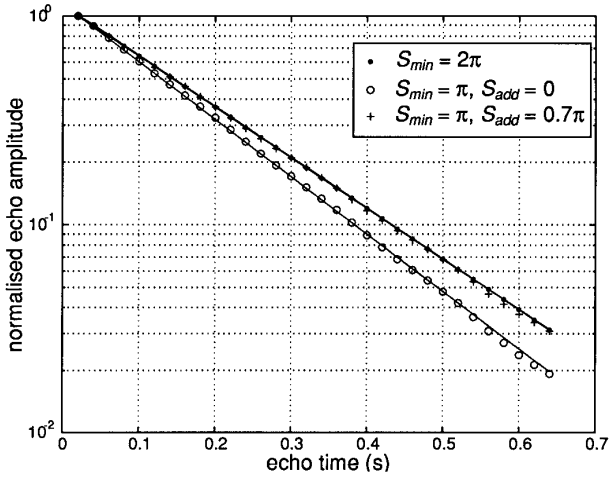

FIG. 6. Echo magnitudes from 32 echo bulk-magnetization simulations using the parameters given in Table 1. The optimal case ($S_{\min} = 2\pi$) yields T_{2OBS} = 179.0 ms. With $S_{\min} = \pi$ and no spoiler adjustment ($S_{add} = 0$) T_{2OBS} = 157.9 ms, while with the first spoiler increased by $S_{add} = 0.7\pi$, T_{2OBS} = 178.6 ms.

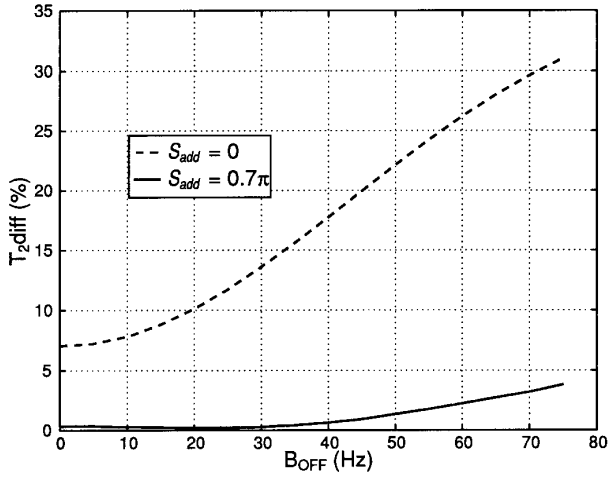

FIG. 8. Difference between T_{2OPT} and T_{2OBS} as a percentage of T_{2OPT} plotted as a function of the offset frequency from resonance of the rf refocusing pulse (B_{OFF}), with amplitude missetting of the rf refocusing pulse (B_{MIS}) held constant at 5%.

Fig. 6. Bulk simulations were also generated to assess the dependence of S_{add} upon imperfection of the rf refocusing pulse due to B_1 amplitude missetting (B_{MIS}) and resonance offset (B_{OFF}) effects; the results are shown in Figs. 7 and 8.

In order to assess how a given S_{add} adjustment affects the T_{2OBS} of samples with various relaxation rates, 32-echo data were simulated using three different R_2 rates, and for each of these up to five different R_1 rates. For each of these simulations $S_{\min} = \pi$ and $S_{add} = 0.7\pi$. Table 2 shows the resulting T_{2OBS} for each of these simulations.

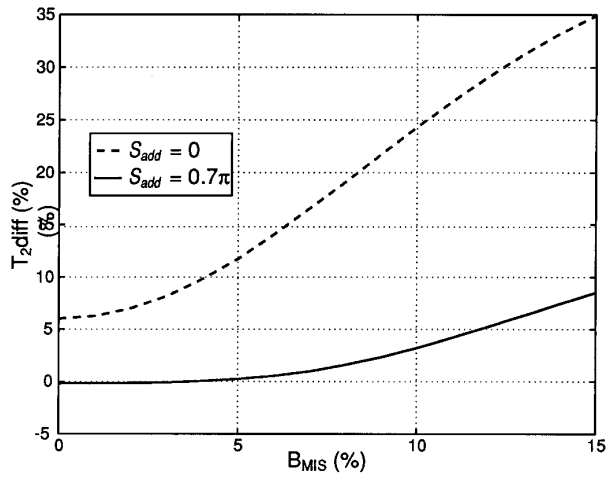

FIG. 7. Difference between T_{2OPT} and T_{2OBS} as a percentage of T_{2OPT} plotted as a function of amplitude missetting of the rf refocusing pulse (B_{MIS}), with the offset frequency from resonance of the rf refocusing pulse (B_{OFF}) held constant at 25 Hz.

Slice Selection Simulations

One factor of an imaging protocol to which S_{add} is sensitive is slice location. The above simulations were performed assuming no offset in the slice direction, in which case the spoiler gradients produce no net phase shift of magnetisation. When imaging with an offset in the slice direction, a spoiler gradient imparts a net phase shift to the transverse magnetization equal to

$$\Omega = \gamma G \Delta \tau, \qquad [1]$$

where G is the gradient amplitude, Δ is the slice offset, and τ is the gradient duration. In the multiecho spoiler pattern employed here (Fig. 1), every spoiler gradient (prior to implementation of S_{add} adjustment) has an amplitude equal to

$$G = \frac{\pm n S_{\min}}{\gamma \delta \tau}, \qquad [2]$$

where δ is the slice thickness and n is an integer. Substituting [2] into [1] yields

$$\Omega = \frac{\pm n S_{\min} \Delta}{\delta}. \qquad [3]$$

Therefore, as long as $S_{\min}\Delta/\delta = \pm 2m\pi$ (m = 1, 2, . . .) no spoiler gradient will impart a nonzero net phase shift. For example, for the case of $S_{\min} = \pi$ slice offsets need to be chosen as an integer multiple of twice the slice thickness. If this constraint is not met, different S_{add} values must be used to minimize the unwanted signal, and the minimal signal

TABLE 2
Observed T_2s from 32 Echo Simulations Using a Range of R_1 and R_2 Values

	T_2 (ms)	T_2 (ms)	T_2 (ms)
True T_2	300.0	100.0	40.0
T_{2OPT}	255.0	94.5	39.1
R_1	T_{2OBS} (ms)	T_{2OBS} (ms)	T_{2OBS} (ms)
0	253.7	94.6	38.9
1	253.3	94.5	38.9
3.33	252.5	94.3	38.9
10	—	94.0	38.9
25	—	—	38.9
Range	0.47%	0.32%	0.00%

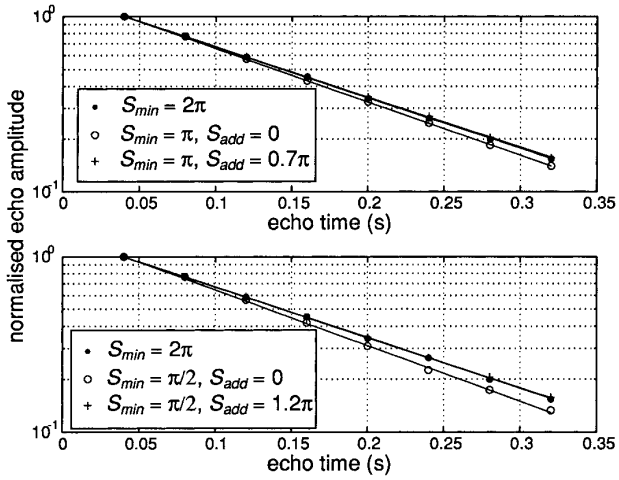

FIG. 10. MRI echo magnitudes from eight echo acquisitions. The optimal case ($S_{min} = 2\pi$) yields $T_{2OBS} = 150.1$ ms (and SNR = 73), compared to the spectroscopically measured value of 163 ms. With $S_{min} = \pi$ (top) and no spoiler adjustment ($S_{add} = 0$) $T_{2OBS} = 142.6$ ms (and SNR = 66), while with the first spoiler increased by $S_{add} = 0.7\pi$ $T_{2OBS} = 151.5$ ms (and SNR = 54). With $S_{min} = \pi/2$ (bottom) and no spoiler adjustment ($S_{add} = 0$) $T_{2OBS} = 136.8$ ms (and SNR = 59), while with the first spoiler increased by $S_{add} = 1.2\pi$ $T_{2OBS} = 150.9$ ms (and SNR = 44).

contribution will not be as low as otherwise found for the case of zero net phase shift. These results are demonstrated in Fig. 9, using coherence pathway simulations, which shows T_1- and phase-artefact contributions to the observed signal for three cases of slice direction offset and the previously shown case of zero offset.

MRI Measurements

Multiecho imaging measurements of a 25 cm diameter cylindrical $MnCl_2$ phantom were made at 3.0 T. The phantom solution relaxation rates were determined spectroscopically to be $T_2 = 163$ ms and $T_1 = 1260$ ms. Eight echoes were collected in a CPMG manner using TE = 40 ms, TR = 1s, 2 NEX add/subtract cycled, and with B_1 intentionally misset by +5% and the resonance frequency offset by +25 Hz. A 1 cm slice was selected with a 1500 Hz bandwidth three-lobe sinc pulse, and refocusing was achieved with 1500 ms hard pulses. The FOV was 80 cm, acquired with 128 samples at a bandwidth of 16.7 kHz and 128 phase-encoding steps. The spoiler gradients were trapazoidal in shape and 4 ms in duration, including 1 ms ramp times. Data were collected for $S_{min} = 2\pi$, π, and $\pi/2$, and for various S_{add} settings; selected results are plotted in Fig. 10. Signal-to-noise ratio (SNR) values listed in the caption are the quotient of the mean and standard deviation of the signal amplitude from a square region of interest contained within the domain of the phantom.

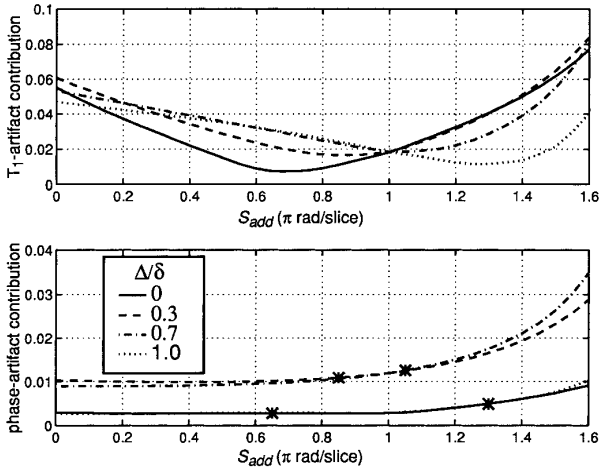

FIG. 9. Mean contribution per echo of magnetization from the T_1- and phase-artefact pathways as a function of the spoiler adjustment, S_{add}, for $S_{min} = \pi$ and four cases of slice offset (Δ) divided by slice thickness (δ).

DISCUSSION

Minimizing Unwanted Signal

From Fig. 2, which demonstrates the dependence of T_{2OBS} on S_{add}, it can be seen that for the four cases of suboptimal spoiler gradients shown there is a S_{add} adjustment that will yield T_{2OBS} equal to T_{2OPT}. However, this does not indicate that at this S_{add} adjustment one is measuring only signal arising from true-T_2 coherence pathways. Therefore, M_{OBS} is broken into M_{T2} and M_{T1}, and the relative amount of corruption from T_1-artefact pathways is plotted in Fig. 3. Inspection of Figs. 2 and 3 reveals that for a given value of S_{min}, the S_{add} adjustment that minimizes M_{T1} relative to M_{OBS} is very near the value of S_{add} required to yield a T_{2OBS} equal to T_{2OPT}. These two values are not exactly equal because the T_1-artefact contribution is not reduced completed to zero (Fig. 5b), so at the point of minimum T_1-artefact contribution there is still some contamination of M_{OBS}.

If phase-artefacts were not a problem it would appear that

even for values of S_{min} as low as $\pi/4$ an appropriate S_{add} adjustment would reduce the mean contribution of M_{T1} to $<2\%$ per echo and result in a T_{2OBS} very near T_{2OPT} ($\approx 1\%$ low for $S_{min} = \pi/4$, $S_{add} = 1.6\pi$). However, in general, the observed signal will be further corrupted by the ghost image arising from phase-artefact pathways. Similar to Fig. 3, Fig. 4 shows the relative (potential) contribution of M_P to M_{OBS}. While there are S_{add} adjustments that will reduce this contribution to approximately 2% per echo in all four S_{min} cases shown, these S_{add} values do not correspond to the S_{add} values prescribed from Fig. 3 which are identified in Fig. 4 by asterisks. Figures 3 and 4 together indicate that for $S_{min} = \pi/4$ the combination of M_{T1} and M_P cannot be reduced below an average of $\approx 12\%$ per echo, while for $S_{min} \geq \pi$, the combined corrupting contribution can be reduced to average less than 1% per echo.

With the incorporation of additional phase-encoding (rewind) gradients in the spin-echo sequence (8) to bring the ghost image in phase with the true-T_2 and T_1-artefact images it may appear possible to achieve somewhat better correction, although at the expense of somewhat increased echo times. However, the rewind gradients do not remove phase-artefact signal, but rather convert it to T_1-artefact signal. This is an effective method of removing image ghosts, but will not eliminate the corrupting phase-artefact signal.

The mechanism by which the corrupting signal is reduced is demonstrated in Fig. 5. With $S_{min} = \pi$ and no spoiler adjustment, 16 unwanted coherence pathways are found to contribute significantly to the eighth echo and their amplitudes are plotted in Fig. 5 (top). The net signal from these 16 unwanted pathways represents 10.5% of the observed echo magnitude. With the spoiler adjustment of $S_{add} = 0.7\pi$, the number of contributing unwanted pathways jumps to 28, as shown in Fig. 5 (bottom), but the net signal from these pathways drops to 2.2% of the observed echo because of an increased mutual cancellation of unwanted signals.

Factors Affecting S_{add}

For relatively small NE values it is practical to perform coherence pathway simulations that will yield plots similar to those in Figs. 2–4 from which it is possible to determine the optimal S_{add} for a given imaging protocol and rf refocusing pulse imperfections. However, for large NE, due to the large number of coherence pathways, reliance must be made upon bulk simulations which cannot determine S_{add} explicitly because only M_{OBS} can be computed. If the S_{add} value required to minimise unwanted signal were sensitive to the number of echoes, determining the best S_{add} setting could prove problematic. However, as demonstrated in Fig. 6, this is not the case. With 32 echoes and $S_{min} = \pi$, an S_{add} value of 0.7π, the same value that was used with NE = 8, results in echo magnitudes very close to those resulting from the optimal case of $S_{min} = 2\pi$. Also, as seen in Table 2, results from simulations using the same spoiler setting showed that over a wide range of biologically relevant R_1 and R_2 values T_{2OBS} was very near T_{2OPT}, suggesting a near maximal reduction of net signal from unwanted coherence pathways. Therefore, the best S_{add} value for a given multiecho imaging protocol does not appear to be particularly sensitive to NE or relaxation rates.

The sensitivity of S_{add} to B_{OFF} and B_{MIS} is another potential problem in implementing an S_{add} adjustment. Knowing the characteristics of the rf coil and the refocusing pulse being used will provide an estimate of the potential B_{MIS}, as the linewidth will provide an estimate of the effective B_{OFF}, but in practice it is impossible to know precisely B_{OFF} and B_{MIS}, particularly as they vary spatially. If a composite refocusing pulse is used, one might expect as little as $\approx 5\%$ variation in effective B_1 amplitude throughout a volume (9); Fig. 7 indicates that with up to $\pm 5\%$ missetting of B_1 (given $B_{OFF} = 25$ Hz) there is virtually no additional cost in using suboptimal spoiler gradients with the S_{add} adjustment. This does not mean that T_{2OBS} will not vary over a $\pm 5\%$ range of B_{MIS}, but only that over such a range T_{2OBS} will remain as accurate as possible (i.e., $\approx T_{2OPT}$) given the particular B_{MIS}. For comparison, also shown in Fig. 7 is the corresponding T_2 error when suboptimal spoilers are implemented without the adjustment, which demonstrates a much greater sensitivity to B_{MIS}. Similar results for the case of B_{OFF} variation (given $B_{MIS} = 5\%$) are plotted in Fig. 8. Thus, for a reasonably wide range of B_{MIS} and B_{OFF} values it is expected that near optimal T_2 values can be measured using the appropriate S_{add} adjustment determined from coherence pathway simulations.

It should be noted, however, that the sensitivity of S_{add} to rf inaccuracies becomes significantly greater with decreasing S_{min} values. This is due to the fact that the M_{T1} minima (Fig. 3) become much narrower with decreasing S_{min}, which results in the increasing slopes of the T_{2OBS} curves seen in Fig. 2. Thus, at lower settings of S_{min}, small missettings of S_{add} will result in greater increases in M_{T1} contribution to the echo and, in turn, greater differences between T_{2OBS} and T_{2OPT}.

Finally, one must consider the signal-to-noise cost of implementing the S_{add} adjustment, because, while providing additional dephasing to unwanted pathways, S_{add} is also dephasing the desired signal. For $S_{add} = 1.2\pi$, which would be required for the case of $S_{min} = \pi/2$, approximately 50% of the observed signal is lost. This value drops significantly, however, to less than 20% when S_{add} is reduced to 0.7π, corresponding to the case of $S_{min} = \pi$. In most situations, a 20% signal loss is probably a tolerable cost for reducing gradient demands by nearly a factor of 2. Further, it should be pointed out that the SNR of multiecho data acquired used the spoiler adjustment will also be affected by the phase-artefact contribution and the nonlinear phase distribution resulting from the selective excitation pulse, although these factors are not thoroughly investigated in this work.

CONCLUSION

Using computer simulations and experimental data we have demonstrated that when suboptimal spoiler gradients of $S_{min} \geq \pi/2$ are used in multiecho imaging sequences designed to measure T_2, increasing the strength of the first spoiler gradient by the appropriate amount reduces the contamination from unwanted coherence pathways by a factor of several times. With this reduction of corrupting signal, ensuing T_2 measurements are typically within 1% of those obtained using optimal spoiler gradient strengths. With NE = 8, the use of the suboptimal spoiler gradient of $S_{min} = \pi/2$ with an appropriate adjustment gradient S_{add} reduces the maximum spoiler gradient strength required by $\approx$60%, this value approaching 75% with increasing NE. Correction for values of $S_{min} < \pi/2$ is restricted by the ghost image that arises from phase-artefact pathways and reduced signal intensity. Coherence pathway simulations have shown that the effect of the additional spoiler gradient S_{add} is to cause an increase in mutual cancellation of unwanted signals arising from deleterious coherence pathways.

Computer simulations have shown that the optimal adjustment S_{add} for a given suboptimal gradient strength does not depend significantly upon R_1 and R_2 relaxation times or upon a reasonably wide range of rf refocusing pulse missetings. However, the sensitivity of S_{add} to rf inaccuracies increases with decreasing values of S_{min}. As well, the ability of the S_{add} adjustment to reduce unwanted signal is sensitive to the slice location, being optimal for slices in which each unadjusted spoiler gradient produces a net phase shift of $\pm 2m\pi$ $(m = 1, 2, \ldots)$.

ACKNOWLEDGMENTS

The authors acknowledge infrastructural support from the In-Vivo NMR Facility of the University of Alberta and thank the Medical Research Council of Canada for funding.

REFERENCES

1. A. P. Crawley and R. M. Henkelman, *Magn. Reson. Med.* **4,** 34–47 (1987).
2. C. S. Poon and R. M. Henkelman, *J. Magn. Reson. Imag.* **2,** 541–553 (1992).
3. G. J. Barker and T. H. Mareci, *J. Magn. Reson.* **83,** 11–28 (1989).
4. J. Simbrunner, *J. Magn. Reson. A* **109,** 117–120 (1994).
5. R. Kaiser, E. Bartholdi, and R. R. Ernst, *J. Chem. Phys.* **60,** 2966–2979 (1974).
6. D. E. Woessner, *J. Chem. Phys.* **34,** 2057–2061 (1961).
7. J. F. Shen and J. K. Sauders, *J. Magn. Reson.* **96,** 381–386 (1992).
8. Y. Zur, X. Zou, and L. J. Neuringer, *Magn. Reson. Med.* **19,** 464–469 (1991).
9. C. S. Poon and R. M. Henkelman, *J. Magn. Reson.* **99,** 45–55 (1992).